Temporal Correlations of the Running Maximum of a Brownian Trajectory

Olivier Bénichou,[1] P. L. Krapivsky,[2] Carlos Mejía-Monasterio,[3] and Gleb Oshanin[1,*]

[1]*Laboratoire de Physique Théorique de la Matière Condensée, UPMC, CNRS UMR 7600,*
Sorbonne Universités, 4 Place Jussieu, 75252 Paris Cedex 05, France
[2]*Department of Physics, Boston University, Boston, Massachusetts 02215, USA*
[3]*Laboratory of Physical Properties, Technical University of Madrid, Avenida Complutense s/n, 28040 Madrid, Spain*

We study the correlations between the maxima m and M of a Brownian motion (BM) on the time intervals $[0, t_1]$ and $[0, t_2]$, with $t_2 > t_1$. We determine the exact forms of the distribution functions $P(m, M)$ and $P(G = M - m)$, and calculate the moments $\mathbb{E}\{(M - m)^k\}$ and the cross-moments $\mathbb{E}\{m^l M^k\}$ with arbitrary integers l and k. We show that correlations between m and M decay as $\sqrt{t_1/t_2}$ when $t_2/t_1 \to \infty$, revealing strong memory effects in the statistics of the BM maxima. We also compute the Pearson correlation coefficient $\rho(m, M)$ and the power spectrum of M_t, and we discuss a possibility of extracting the ensemble-averaged diffusion coefficient in single-trajectory experiments using a single realization of the maximum process.

Brownian motion (BM) is a paradigmatic stochastic process [1–4] with innumerable applications in physics and chemistry [5,6], biology [7], computer science [8], mathematical finance [9,10], etc. Much effort has been invested in understanding the extreme value statistics (EVS) of BM, e.g., maximal or minimal displacements, spans, survival probabilities, persistence, and various first-passage-time characteristics. Such results appear in numerous studies, see, e.g., Refs. [11–32] emphasizing the relevance of the EVS in diverse physical phenomena.

To the best of our knowledge, nothing is known about temporal correlations of different extremes of BM, although it is interesting to probe how a maximum (minimum) achieved on a certain time interval is correlated to an extremum achieved on a longer time interval, how the span is correlated at different time moments, how the first and the subsequent passage times depend on each other, etc. Here we address these conceptually important questions focusing on the running maximum $M_t = \max_{0 \leq s \leq t} B_s$ of a one-dimensional BM trajectory B_s with $B_0 = 0$. We briefly write

$$m = \max_{0 \leq s \leq t_1} B_s, \qquad M = \max_{0 \leq s \leq t_2} B_s, \qquad t_1 < t_2$$

for the maxima achieved on the time interval $[0, t_1]$ and a longer time interval $[0, t_2]$ (see Fig. 1). Our main goals are to determine $P(m, M)$, the joint probability distribution function (PDF) of the maxima, and the PDF $P(G)$ of the gap $G = M - m$ between the maxima. These PDFs allow us to calculate the cross-moments $\mathbb{E}\{m^l M^k\}$, with arbitrary integers l and k, and the moments $\mathbb{E}\{(M - m)^k\}$ of arbitrary order $k > 0$. We will show that m and M decouple on much larger time scales than the positions of the BM, revealing strong memory effects in the EVS of the BM. Using our results we extract the Pearson correlation

coefficient and determine the power spectrum of M_t. Finally, we discuss the possibility of extracting the ensemble-averaged diffusion coefficient D in single-trajectory experiments using a single realization of M_t.

We start by summarizing a few key properties of M_t which we shall need. Denote by $Q_t(M)$ the PDF of the maximum M of BM on $[0, t]$. This PDF is the one-sided Gaussian distribution (see, e.g., [1–3])

$$Q_t(M) = \frac{1}{\sqrt{\pi D t}} \exp\left(-\frac{M^2}{4Dt}\right). \tag{1}$$

Using (1) one can express the moments $\mathbb{E}\{M_t^k\}$, with arbitrary $k > -1$, through the gamma function

$$\frac{\mathbb{E}\{M_t^k\}}{(4Dt)^{k/2}} = \Gamma\left(\frac{k+1}{2}\right)/\sqrt{\pi}. \tag{2}$$
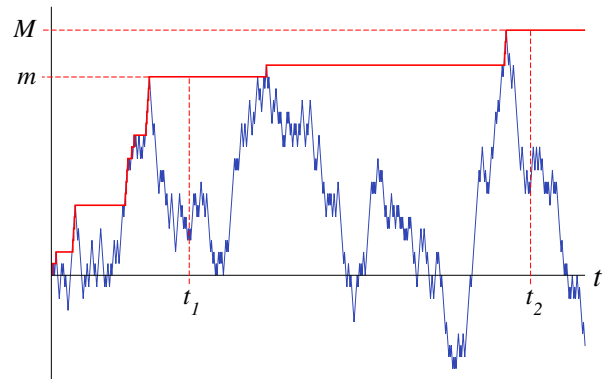

FIG. 1. A realization of a BM (blue) and the corresponding maximum process M_t (red). M and m are the maxima of BM on $[0, t_2]$ and $[0, t_1]$, respectively.

Next, let $\Pi_t(M, x)$ be the PDF that the BM is at x at time t and it has achieved the maximum M during the time interval $[0, t]$. This PDF reads (see, e.g., [1–3])

$$\Pi_t(M, x) = \frac{2M - x}{2\sqrt{\pi D^3 t^3}} \exp\left(-\frac{(2M - x)^2}{4Dt}\right). \qquad (3)$$

To determine the joint PDF $P(m, M)$ we will need an auxiliary probability $S_t(m)$ that the BM will not reach a fixed level $m > 0$ within the time interval $[0, t]$. This probability is well known [1–4],

$$S_t(m) = \mathrm{erf}\left(\frac{m}{\sqrt{4Dt}}\right). \qquad (4)$$

Here $\mathrm{erf}(\cdot)$ is the error function. The joint PDF $P(m, M)$ can be expressed as the sum of two contributions. The first is due to trajectories B_s which reach a maximal value m for $s \in [0, t_1]$, appear at some position $x \le m$ at $s = t_1$, and then reach a maximal value $M > m$ for $s \in [t_1, t_2]$ (see Fig. 2); the second is due to trajectories B_s which reach a maximal value m for $s \in [0, t_1]$, appear at some position $x \le m$ at $s = t_1$, and in the following time interval $s \in [t_1, t_2]$ do not reach m again, so that $M = m$. We thus formally represent $P(m, M)$ as

$$P(m, M) = \int_{-\infty}^{m} dx \Pi_{t_1}(m, x) Q_{t_2 - t_1}(M - x)$$
$$+ \delta(M - m) \int_{-\infty}^{m} dx \Pi_{t_1}(m, x) S_{t_2 - t_1}(m - x). \qquad (5)$$

Using the definitions in (1), (3), and (4), and performing the integrals in (5), we find the following exact result:
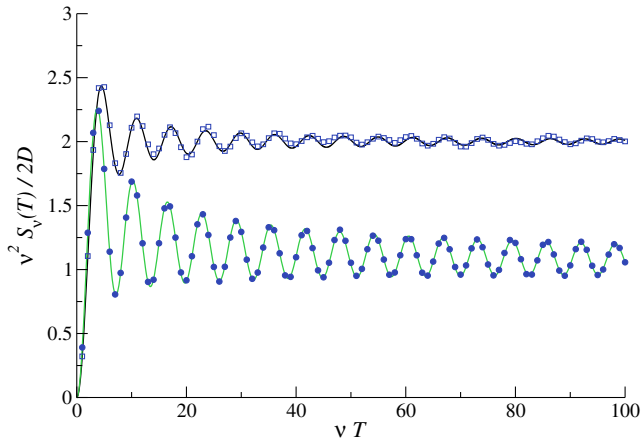
FIG. 2. Comparison of the power spectra of the maximum process [solid line, (15)] and $S_\nu^{(BM)}(T)$ for the BM (dashed line). Symbols denote the results of Monte Carlo (MC) simulations.

$$P(m, M) = \frac{(2m - M)}{2\sqrt{\pi D^3 t_2^3}} \exp\left(-\frac{(M - 2m)^2}{4Dt_2}\right)$$
$$\times \mathrm{erfc}\left(\sqrt{\frac{t_2 - t_1}{Dt_1 t_2}} \frac{m}{2} + \sqrt{\frac{t_1}{Dt_2(t_2 - t_1)}} \frac{(M - m)}{2}\right)$$
$$+ \frac{1}{\pi Dt_2} \sqrt{\frac{t_2 - t_1}{t_1}} \exp\left(-\frac{m^2}{4Dt_1} - \frac{(M - m)^2}{4D(t_2 - t_1)}\right)$$
$$+ \frac{\delta(M - m)}{\sqrt{\pi Dt_2}} \exp\left(-\frac{m^2}{4Dt_2}\right) \mathrm{erfc}\left(\sqrt{\frac{t_2 - t_1}{Dt_1 t_2}} \frac{m}{2}\right),$$
$$\qquad (6)$$

where $\mathrm{erfc}(\cdot)$ is the complementary error function.

Equation (6) is our central result, which allows for a direct calculation of all other properties of interest. For instance, using (6) we determine $P(G)$, the probability density that $M - m = G \ge 0$,

$$P(G) = \frac{2}{\pi} \arcsin\left(\sqrt{\frac{t_1}{t_2}}\right) \delta(G)$$
$$+ \frac{e^{-G^2/(4Dt_2)}}{\sqrt{\pi Dt_2}} \mathrm{erfc}\left(\sqrt{\frac{t_1}{Dt_2(t_2 - t_1)}} \frac{G}{2}\right). \qquad (7)$$

The PDF of the gap between the first- and the second-ordered maxima of a BM (a different quantity from the one we consider) has been analyzed in Ref. [28].

Next, we determine the cross-moments of the maxima m and M by simply integrating $P(m, M)$ in (6),

$$\frac{\mathbb{E}\{m^l M^k\}}{(4Dt_2)^{(l+k)/2}}$$
$$= \frac{z^{(k+l)/2}}{\pi} \left[\sum_{n=0}^{k} \binom{k}{n} \Gamma\left(\gamma - \frac{n}{2}\right)\right.$$
$$\times \Gamma\left(\frac{n+1}{2}\right)\left(\frac{1 - z}{z}\right)^{n/2} - \frac{k 2^k \Gamma(\gamma + \frac{1}{2})}{4\gamma}(1 - z)^\gamma$$
$$\times \sqrt{z} \sum_{n=0}^{k-1} \binom{k-1}{n} \sum_{p=0}^{l} \binom{l}{p} \frac{(z - 1/2)^n z^p Q_{n,p}}{(1 - z)^{2\mu}(\gamma - \mu)}\right], \qquad (8)$$

with

$$Q_{n,p} = \frac{\gamma}{\mu} {}_2F_1\left(\gamma + \frac{1}{2}, \mu; \mu + 1; \frac{z}{z - 1}\right)$$
$$+ \frac{(-1)^{n+p}\gamma}{\mu}\left(\frac{1 - z}{z}\right)^{2\mu} {}_2F_1\left(\gamma + \frac{1}{2}, \mu; \mu + 1, \frac{z - 1}{z}\right)$$
$$- (-1)^{n+p}\left(\frac{1 - z}{z}\right)^{2\mu} {}_2F_1\left(\gamma + \frac{1}{2}, \gamma; \gamma + 1; \frac{z - 1}{z}\right)$$
$$- {}_2F_1\left(\gamma + \frac{1}{2}, \gamma; \gamma + 1; \frac{z}{z - 1}\right), \qquad (9)$$

where ${}_2F_1$ denotes the hypergeometric function and

$$\gamma = \frac{k+l+1}{2}, \qquad \mu = \frac{n+p+1}{2}, \qquad z = \frac{t_1}{t_2}.$$

The first few cross-moments read

$$\frac{\mathbb{E}\{mM\}}{2Dt_2} = \frac{z}{2} + \frac{\sqrt{z(1-z)}}{\pi} + \frac{1}{\pi}\arcsin(\sqrt{z}),$$

$$\frac{\mathbb{E}\{mM^2\}}{(4Dt_2)^{3/2}} = \frac{z^{3/2} + 3\sqrt{z} + 2 - 2(1-z)^{3/2}}{6\sqrt{\pi}},$$

$$\frac{\mathbb{E}\{m^2M\}}{(4Dt_2)^{3/2}} = \frac{2z^{3/2} + 1 - (1-z)^{3/2}}{3\sqrt{\pi}},$$

$$\frac{\mathbb{E}\{m^2M^2\}}{8(Dt_2)^2} = \frac{z(1+z)}{2} + \frac{(2z-1)\sqrt{z(1-z)}}{\pi}$$
$$+ \frac{1}{\pi}\arcsin(\sqrt{z}). \tag{10}$$

To highlight the decay of correlations between m and M when $t_2 \to \infty$ and t_1 is kept fixed, we formally rewrite [taking advantage of (2)] the first expression in (10) as

$$\frac{\mathbb{E}\{mM\}}{\mathbb{E}\{m\}\mathbb{E}\{M\}} = 1 + \frac{\pi}{4}\sqrt{z} + O(z), \tag{11}$$

implying that correlations decouple slowly, as $\sqrt{t_1/t_2}$.

From (7) we find the moments of the gap

$$\frac{\mathbb{E}\{G^k\}}{(4Dt_2)^{k/2}} \equiv \frac{\mathbb{E}\{(M-m)^k\}}{(4Dt_2)^{k/2}} = \frac{\Gamma(\frac{k+1}{2})}{\sqrt{\pi}}$$
$$- \frac{k\Gamma(\frac{k}{2})\sqrt{z}(1-z)^{(k+1)/2}}{\pi} {}_2F_1\left(1, \frac{k}{2}+1; \frac{3}{2}; z\right) \tag{12}$$

for arbitrary $k > -1$. For example, for $k = 2$ we have

$$\mathbb{E}\{(M-m)^2\} = \frac{4Dt_2}{\pi}(\arccos(\sqrt{z}) - \sqrt{z(1-z)})$$
$$= \mathbb{E}\{M^2\}\left[1 - \frac{4}{\pi}\sqrt{z} + O(z^{3/2})\right], \tag{13}$$

which implies that the memory of m fades as $\sqrt{t_1/t_2}$. The correlations between positions of the BM itself, $\mathbb{E}\{(B_{t_2} - B_{t_1})^2\} = \mathbb{E}\{B_{t_2}^2\}(1 - t_1/t_2)$, decay much faster. Because ${}_2F_1(a, b; c; z) \to 1$ when $z \to 0$, Eq. (12) yields $\mathbb{E}\{G^k\}/\mathbb{E}\{M^k\} = 1 + O(\sqrt{t_1/t_2})$ for any $k > -1$ and $t_1/t_2 \ll 1$.

We consider several direct applications of our exact results.

(i) First, we calculate the Pearson's coefficient $\rho = \text{Cov}(m, M)/\sqrt{\text{Var}(m)\text{Var}(M)}$ which is a measure of the linear correlation between m and M,

$$\rho = \frac{\left(\frac{\pi}{2}\sqrt{z} - 2 + \sqrt{1-z} + \frac{\arcsin(\sqrt{z})}{\sqrt{z}}\right)}{\pi - 2}. \tag{14}$$

We observe that ρ is a monotonically increasing function of z and that $\rho \geq \rho_{\text{BM}}(B_{t_1}, B_{t_2}) \equiv \sqrt{z}$, where ρ_{BM} is the Pearson coefficient for the BM, which again implies that M_t is more strongly correlated than the BM itself.

(ii) Further, for the power spectrum $S_\nu(T)$ of M_t we get

$$S_\nu(T) = \frac{1}{T}\mathbb{E}\left\{\left|\int_0^T e^{i\nu t}M_t dt\right|^2\right\}$$
$$= \frac{2D}{\nu^2}\left[1 - \frac{\sin(\nu T)}{\nu T} + 2\sin\left(\frac{\nu T}{2}\right)J_1\left(\frac{\nu T}{2}\right)\right], \tag{15}$$

where $J_1(\cdot)$ is the Bessel function. This result (valid for any ν and T) can be compared with the power spectrum of the BM, $S_\nu^{(BM)}(T) \equiv 4D[1 - \sin(\nu T)/\nu T]/\nu^2$ (see Fig. 2). Despite strong correlations and an intermittent character of the maximum process M_t, its limiting power spectrum $S_\nu = \lim_{T\to\infty} S_\nu(T) = 2D/\nu^2$ exhibits the same ν^{-2} decay as the BM, but the amplitude is 2 times smaller. This limit, however, is approached as $1/\sqrt{T}$, as compared to the $1/T$ relaxation taking place for the BM. Indeed, for M_t we observe much stronger oscillations than for the BM (see Fig. 2).

(iii) Finally, we inquire about a possibility of extracting the ensemble-averaged diffusion coefficient D from a single realization of the maximum process M_t. Recently, much effort has been invested in understanding how to do this using B_s itself; see, e.g., [33–39]. In particular, it was realized that a time-averaged functional of the form

$$D_{\text{msd}} = \frac{1}{2\tau(T-\tau)}\int_0^{T-\tau} dt(B_{t+\tau} - B_t)^2, \tag{16}$$

where $\tau > 0$ is the time lag and T the total observation time, is an efficient estimator of D. The point is that for the BM the variance $\text{Var}(D_{\text{msd}})$ of the estimator (16) vanishes with the observation time as $1/T$ (see, e.g., [35]), which means that for any realization of B_t the estimator converges to D with probability 1 as $T \to \infty$.

On the other hand, if the BM takes place in bounded microdomains, i.e., in cells, the limit $T \to \infty$ cannot be taken safely because B_t will start to feel the confinement at a certain moment and D_{msd} will probe the finite-size rather than D. It means that the observation has to be interrupted at some T when the variance of D_{msd} is still finite. In this regard, it may be useful to have other tools to deduce D that will work reliably at short T.

Here we present an example of the estimator of D that uses M_t instead of B_t itself, and has a variance that is independent of T and can be made arbitrarily small (e.g., smaller than experimental blur) by an appropriate tuning of some control parameter. We note also that using M_t instead of B_s has a number of advantages: (i) such an approach requires less data—keeping track of B_t creates a set of size

$\sim T$, while in the case of M_t one has to record only the events when M_t changes its value, which, on average, happens only $\sqrt{T}$ times [27]; (ii) one may expect [40] that the estimators of D based on a single realization of M_t are less "noisy" than those based on B_t, because M_t already filters a great deal of fluctuations of B_t (see Fig. 1).

Let B_s be a projection of an experimentally tracked d-dimensional Brownian trajectory $\mathbf{B}_s$ on one of the axes, and denote by M_t the running maximum of this projection B_s. Suppose we want to fit a random curve M_t^k, where k is a positive number, by some deterministic curve using the least-squares approximation. A natural choice of the deterministic curve is provided by Eq. (2) in which we replace D by an estimated "diffusion coefficient" D_{es}. We construct then a functional of squared residuals,

$$F = \int_0^T \left[M_t^k - \Gamma\left(\frac{k+1}{2}\right) \frac{(4D_{es}t)^{k/2}}{\sqrt{\pi}} \right]^2 dt \quad (17)$$

Regarding D_{es} as an optimization parameter, we minimize F and find the minimum

$$f_k \equiv D_{es}^{k/2} = \frac{\sqrt{\pi}(\frac{k}{2}+1)}{2^k \Gamma(\frac{k+1}{2}) T^{k/2+1}} \int_0^T M_t^k dt \quad (18)$$

providing us with a k-parametrized family of estimators minimizing an error in the least-squares fitting of M_t^k of a given realization of M_t. While the ensemble-averaged value is $\mathbb{E}\{f_k\} \equiv D^{k/2}$, f_k fluctuates around this value giving an estimate $D_{es}^{k/2}$ of the actual value $D^{k/2}$. To quantify the fluctuations of f_k we use Eq. (8) to compute [41] the variance of f_k

$$\frac{\mathrm{Var}(f_k)}{D^k} = \frac{\sqrt{\pi}(k+2)(3k+2)\Gamma(k+1/2)}{\{4\Gamma[(k+3)/2]\}^2} - 1. \quad (19)$$

Numerical simulations indicate the validity of (19) for non-negative, not necessarily integer, values of k (see Fig. 3). Inspecting Eq. (19), we observe that $\mathrm{Var}(f_k)$ is a nonmonotonic (for $D < 1/2$) function of k which vanishes when $k \to 0$ or $k \to \infty$, suggesting that we have to take either very small or very big values of k in order to minimize the error of the estimator in Eq. (18). We have not been able to determine the distribution $P(f_k)$, so we resorted to numerical analysis to get the variance of the nonlinearly transformed variable $D_{es} = f_k^{2/k}$. The results of our MC simulations (Fig. 4) show that $\mathrm{Var}(D_{es})$ is a nonmonotonic function of k and it is indeed advantageous to use big values of k for which this variance can be made arbitrarily small.

The variance $\mathrm{Var}(D_{es})$ is independent of time, yet in practice one records the trajectory B_t at discrete time moments; in this case $\mathrm{Var}_N(D_{es})$ starts to depend on the number N of recorded points, attaining the limiting value $\mathrm{Var}(D_{es})$ when $N \to \infty$. In the inset to Fig. 4 we plot the results of the MC simulations for the deviation $\delta^2(D_{es}) = [\mathrm{Var}(D_{es}) - \mathrm{Var}_N(D_{es})]/D^2$ as a function of N for several
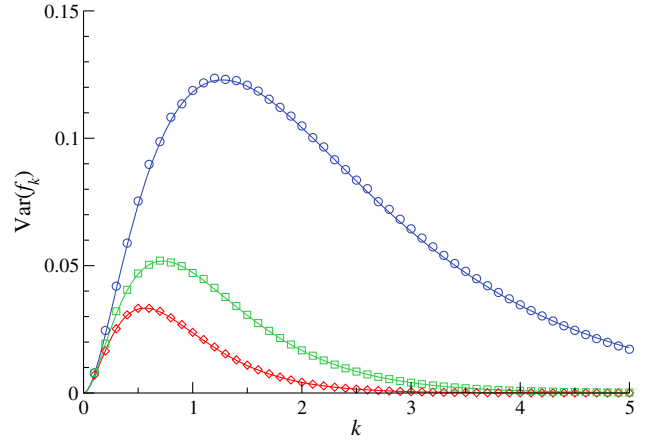

FIG. 3. The variance of f_k as a function of k for $D = 0.25$, $D = 0.01$, and $D = 0.005$ (from top to bottom). Solid lines are Eq. (19) with k considered as a continuous variable, while the symbols are the results of the MC simulations.

values of the control parameter k. We observe that the curves corresponding to different values of k collapse when we plot $k^2\sqrt{N}\delta^2(D_{es})$, implying that $\delta^2(D_{es}) \sim c/(k^2\sqrt{N})$, where c is a constant of order of unity. Thus, the error stemming out of a finite N can be made arbitrarily small by choosing a sufficiently large value of k.

Finally, in Fig. 5 we compare the variance of the commonly used estimator in Eq. (16) against the variance of the estimator D_{es}, based on M_t. We observe that at short times the latter is much smaller, which supports our guess that the ensemble-averaged diffusion coefficient D can be reliably deduced from estimators based on M_t. Seeking other estimators based on extremal properties of B_t that possess an ergodic property suggests an interesting new field of research.
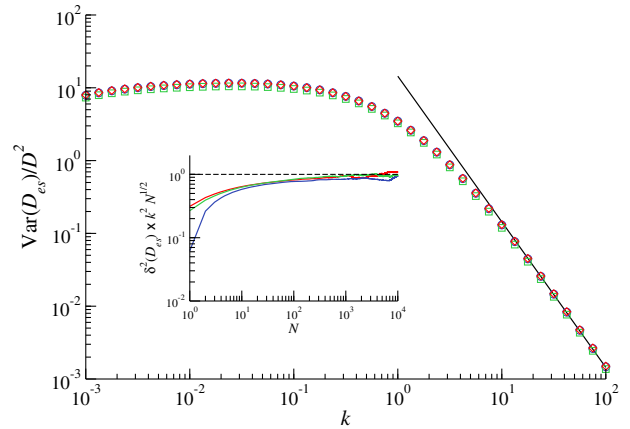

FIG. 4. $\mathrm{Var}(D_{es} = f_k^{2/k})/D^2$ using a nonlinearly transformed estimator in Eq. (18) as a function of k for $D = 0.25$, $D = 0.01$, and $D = 0.005$ (from top to bottom). The solid line is $1/k^2$. The inset shows the dependence of the deviation $\delta^2(D_{es})$ (see the text) on the number N of recorded points of a discretized trajectory. Different colors correspond to $k = 10$ (blue), $k = 50$ (green), and $k = 10^2$ (red).
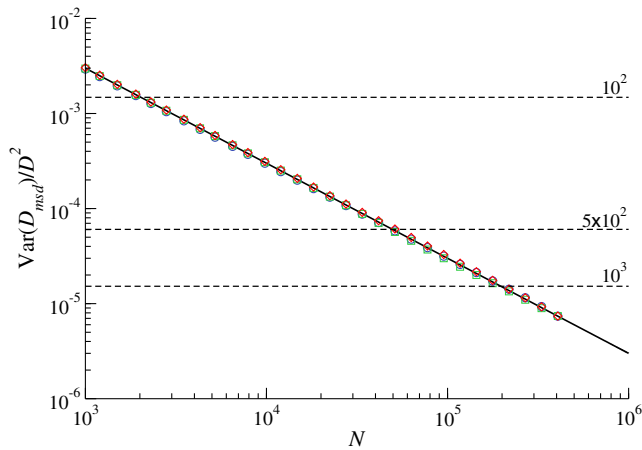
FIG. 5. The variance of the discretized time-averaged functional in Eq. (16), divided by D^2, versus the number N of recorded positions of the trajectory B_t. The solid line is the theoretical result, $\mathrm{Var}(D_{\mathrm{msd}})/D^2 \sim 3/N$, while the symbols (the same as in Figs. 3 and 4) are results of MC simulations for $D = 0.25$, $D = 0.01$, and $D = 0.005$. The horizontal dashed lines give $\mathrm{Var}(D_{\mathrm{es}})/D^2$ for $k = 10^2$, 5×10^2, and 10^3.

*Corresponding author.
  oshanin@lptmc.jussieu.fr

 [1] P. Lévy, *Processus Stochastiques et Mouvement Brownien* (Gauthier-Villars, Paris, 1948).
 [2] K. Itô and H. P. McKean, *Diffusion Processes and Their Sample Paths* (Springer, New York, 1965).
 [3] P. Mörters and Y. Peres, *Brownian Motion* (Cambridge University Press, Cambridge, England, 2010).
 [4] S. Redner, *A Guide to First-Passage Processes* (Cambridge University Press, Cambridge, England, 2001).
 [5] R. Metzler and J. Klafter, Phys. Rep. **339**, 1 (2000).
 [6] P. L. Krapivsky, S. Redner, and E. Ben-Naim, *A Kinetic View of Statistical Physics* (Cambridge University Press, Cambridge, England, 2010).
 [7] H. C. Berg, *Random Walks in Biology* (Princeton University Press, Princeton, NJ, 1993).
 [8] S. N. Majumdar, Curr. Sci. **89**, 2076 (2005).
 [9] R. J. Williams, *Introduction to the Mathematics of Finance* (American Mathematical Society, Providence, 2006).
[10] R. Chicheportiche and J.-P. Bouchaud, in *First-Passage Phenomena and Their Applications*, edited by R. Metzler, G. Oshanin, and S. Redner (World Scientific Publishers, Singapore, 2014).
[11] K. Lindenberg and B. J. West, J. Stat. Phys. **42**, 201 (1986).
[12] P. L. Krapivsky and S. Redner, Am. J. Phys. **64**, 546 (1996).
[13] G. Schehr and P. Le Doussal, J. Stat. Mech. (2010) P01009.
[14] A. J. Bray, S. N. Majumdar, and G. Schehr, Adv. Phys. **62**, 225 (2013).
[15] S. Condamin, O. Bénichou, and M. Moreau, Phys. Rev. Lett. **95**, 260601 (2005).
[16] S. Condamin, O. Bénichou, and J. Klafter, Phys. Rev. Lett. **98**, 250602 (2007).
[17] M. Sheinman, O. Bénichou, R. Voituriez, and Y. Kafri, J. Stat. Mech. (2010) P09005.
[18] C. Mejía-Monasterio, G. Oshanin, and G. Schehr, J. Stat. Mech. (2011) P06022.
[19] S. Condamin, O. Bénichou, V. Tejedor, R. Voituriez, and J. Klafter, Nature (London) **450**, 77 (2007).
[20] O. Bénichou and R. Voituriez, Phys. Rep. **539**, 225 (2014).
[21] G. Oshanin and S. Redner, Europhys. Lett. **85**, 10008 (2009).
[22] G. Oshanin, A. Rosso, and G. Schehr, Phys. Rev. Lett. **110**, 100602 (2013).
[23] D. S. Dean, S. Gupta, G. Oshanin, A. Rosso, and G. Schehr, J. Phys. A **47**, 372001 (2014).
[24] *First-Passage Phenomena and Their Applications*, edited by R. Metzler, G. Oshanin, and S. Redner (World Scientific Publishers, Singapore, 2014).
[25] T. G. Mattos, C. Mejía-Monasterio, R. Metzler, and G. Oshanin, Phys. Rev. E **86**, 031143 (2012).
[26] A. Perret, A. Comtet, S. N. Majumdar, and G. Schehr, J. Stat. Phys. **161**, 1112 (2015).
[27] S. N. Majumdar and R. M. Ziff, Phys. Rev. Lett. **101**, 050601 (2008).
[28] S. N. Majumdar, P. Mounaix, and G. Schehr, Phys. Rev. Lett. **111**, 070601 (2013).
[29] E. Ben-Naim and P. L. Krapivsky, Phys. Rev. Lett. **113**, 030604 (2014).
[30] E. Ben-Naim, P. L. Krapivsky, and J. Randon-Furling, J. Phys. A **49**, 205003 (2016).
[31] H. Krusemann, A. Godec, and R. Metzler, Phys. Rev. E **89**, 040101(R) (2014).
[32] A. Godec and R. Metzler, Sci. Rep. **6**, 20349 (2016).
[33] M. J. Saxton, Biophys. J. **72**, 1744 (1997).
[34] X. Michalet and A. J. Berglund, Phys. Rev. E **85**, 061916 (2012).
[35] D. S. Grebenkov, Phys. Rev. E **83**, 061117 (2011).
[36] D. S. Grebenkov, Phys. Rev. E **84**, 031124 (2011).
[37] A. Andreanov and D. S. Grebenkov, J. Stat. Mech. (2012) P07001.
[38] D. Boyer, D. S. Dean, C. Mejía-Monasterio, and G. Oshanin, J. Stat. Mech. (2013) P04017.
[39] D. Boyer, D. S. Dean, C. Mejía-Monasterio, and G. Oshanin, Phys. Rev. E **85**, 031136 (2012).
[40] V. Tejedor, O. Bénichou, R. Voituriez, R. Jungmann, F. Simmel, C. Selhuber-Unkel, L. B. Oddershede, and R. Metzler, Biophys. J. **98**, 1364 (2010).
[41] The usage of Eq. (8) limits our analysis to non-negative integer values of k.